https://doi.org/10.5194/acp-2022-278
Preprint. Discussion started: 22 April 2022

Atmospheric Chemistry and Physics Discussions

Effects of the sample matrix on the photobleaching and photodegradation of toluene-derived secondary organic aerosol compounds

Alexandra L. Klodt[1], Marley Adamek[2], Monica Dibley[2], Sergey A. Nizkorodov[1*], Rachel E. O'Brien[2*]

[1]Department of Chemistry, University of California Irvine, Irvine, CA, 92697, USA
[2]Department of Chemistry, William & Mary, Williamsburg, VA, 23187, USA

Correspondence to: Rachel E. O'Brien (reobrien@wm.edu) or Sergey A. Nizkorodov (nizkorod@uci.edu)

Abstract. Secondary organic aerosol (SOA) generated from the photooxidation of aromatic compounds in the presence of oxides of nitrogen is known to efficiently absorb ultraviolet and visible radiation. With exposure to sunlight, the photodegradation of chormophoric compounds in the SOA causes this type of SOA to slowly photobleach. These photodegradation reactions may occur in cloud droplets, which are characterized by low concentrations of solutes, or in aerosol particles, which can have highly viscous organic phases and aqueous phases with high concentrations of inorganic salts. To investigate the effects of the surrounding matrix on the rates and mechanisms of photodegradation of SOA compounds, SOA was prepared in a smog chamber by photooxidation of toluene in the presence of NO_x. The collected SOA was photolyzed for up to 24 h using UV-B radiation (300-400 nm) from a Xenon arc lamp under different conditions: directly on the filter, dissolved in pure water, and dissolved in 1 M ammonium sulfate. The SOA mass absorption coefficient was measured as a function of irradiation time to determine photobleaching rates. Electrospray ionization high resolution mass spectrometry coupled to liquid chromatography separation was used to observe changes in SOA composition resulting from the irradiation. The rate of decrease in SOA mass absorption coefficient due to photobleaching was the fastest in water, with the presence of 1 M ammonium sulfate modestly slowing down the photobleaching. Photobleaching directly on the filter was much slower, and approximately 50% of the absorption persisted even after 5 h of irradiation. The high-resolution mass spectrometry analysis revealed an efficient photodegradation of nitrophenol compounds on the filter but not in the aqueous phases, with relatively little change observed in the composition of the SOA irradiated in water or 1 M ammonium sulfate despite faster photobleaching. This suggests that nitrophenol photodegradation contributes much more significantly to photobleaching in the organic phase than in the aqueous phase. We conclude that the SOA absorption coefficient lifetime with respect to photobleaching and lifetimes of individual chromophores in SOA with respect to photodegradation will depend strongly on the sample matrix in which SOA compounds are exposed to sunlight.

1 Introduction

Brown carbon (BrC) aerosol has important impacts on the Earth's radiative forcing (Feng et al., 2013). Because it absorbs actinic radiation in the near-UV (300 to 400 nm) and visible spectral ranges, BrC aerosol reduces the scattering of solar radiation and cooling effect relative to non-absorbing aerosols (Laskin et al., 2015). BrC aerosol can be produced from biomass burning or various gas-phase or multiphase reactions in the atmosphere (Laskin et al., 2015). The photooxidation of aromatic compounds in the presence of NO_x is a known anthropogenic source of BrC (Ji et al., 2014; Liu et al., 2016; Romonosky et al., 2016). For example, secondary organic aerosol (SOA) formed from toluene is brown in appearance because it contains nitrophenols and other chromophoric species (Jang and Kamens, 2001; Lin et al., 2015).

https://doi.org/10.5194/acp-2022-278
Preprint. Discussion started: 22 April 2022


Atmospheric Chemistry and Physics Discussions

After its formation, the composition and optical properties of BrC continues to slowly change, driven in part by direct and indirect photolysis processes (collectively referred to as "photodegradation" in this paper) (Hems et al., 2021). Studies of BrC aging by exposure to actinic radiation have largely focused on photodegradation processes occurring in cloud-water (Hems et al., 2021), although aerosol particles are estimated to spend about 85% of their lifecycle under non-cloud conditions (Pruppacher and Jaenicke, 1995). Less work has been done on photodegradation of BrC in submicron particles, which can include pockets of concentrated aqueous solutions as well as solid organic and inorganic phases with a limited amount of water in them. Water in deliquesced aerosol particles differs from cloud water in several ways, especially in terms of the concentrations of inorganic ions. While the dominant inorganic species in both aqueous particles and cloud water are generally ammonium and sulfate (Bikkina et al., 2017), aqueous particles have ionic strengths of greater than 1 M as compared to 10^{-5} to 10^{-2} M in cloud water (Herrmann et al., 2015). Photochemical processes occurring in particle phase water may potentially be altered by high concentrations of inorganic species.

Previous work has found complex effects of ionic strength on aqueous photochemistry in solutions meant to mimic deliquesced aerosol particles. These studies have largely looked at changes in the UV and visible absorption spectrum and photodegradation rate of single molecules in the presence of inert salts. In the case of pyruvic acid, the major absorption band red-shifts and grows in peak intensity at increased ionic strength at lower (< 4) pH values (Mekic et al., 2018; Luo et al., 2020). However, the photodegradation rate has been shown to increase when the ionic strength was increased with $NaClO_4$ (Mekic et al., 2018), but decrease when the ionic strength was adjusted with NaCl and $CaCl_2$ (Luo et al., 2020). When similar experiments were conducted for lignin-derived compounds, increasing ionic strength lead to formation of a new major absorption band at longer, more atmospherically relevant, wavelengths (Zhou et al., 2019; Loisel et al., 2021). Similarly to pyruvic acid, photodegradation kinetics were observed to accelerate for acetosyringone in the presence of $NaClO_4$ (Zhou et al., 2019), but decelerate for vanillin in the presence of $NaNO_3$ and Na_2SO_4 (Loisel et al., 2021). To the best of our knowledge, only one study has considered the impact of varying ionic strength on the rate of photochemical reactions of complex mixtures of organics representative of aerosol particles. Ray et al. (2020) irradiated solutions of rice-straw smoldering primary organic aerosol in the presence of NaCl, $NaNO_3$, and Na_2SO_4 to explore anionic effects and ionic strength effects on photo-bleaching kinetics. They found longer lifetimes of absorbing species in the presence of all ionic species studied. From these studies, it seems that the specific ionic species present during photolysis may be important; however, no work has yet been done with photodegradation in the presence of ammonium sulfate at high ionic strengths.

Direct and indirect photolysis has been identified as a potentially important sink for SOA compounds in the condensed-phase environment found in dry organic particles (Romonosky et al., 2016), but there have only been a few studies on this topic. This environment is uniquely different from aqueous solutions in that SOA molecules are in a highly viscous organic matrix, and different photochemical mechanisms operate compared to those acting in water. Early indications that dry SOA is easily broken down by near-UV radiation came from examining production of volatile products of UV-irradiated SOA (Walser et al., 2007; Mang et al., 2008; Pan et al., 2009). Subsequent studies suggested that direct photolysis is an important sink for atmospheric SOA, but focused primarily on low-NO_x terpene ozonolysis SOA and found that peroxide and carbonyl compounds were driving the photochemistry (Henry and Donahue, 2012; Hung et al., 2013; Epstein et al., 2014; Wong et al., 2015; Hodzic et al., 2015; Badali et al., 2015; Krapf et al., 2016). Romonosky et al. (2016) measured the absorption coefficients of a number of SOA types and estimated their photodegradation lifetimes, with strongly light-absorbing SOA predicted to have the shortest lifetimes. Subsequent experiments found that stronger absorption coefficient does not actually translate to faster photodegradation, with SOA from aromatic precursors being more photostable than SOA from terpenes, even though the latter barely absorb near-UV radiation (Malecha and Nizkorodov, 2016; Malecha et al., 2018; Baboomian et al., 2020). While these studies all gave insight

https://doi.org/10.5194/acp-2022-278
Preprint. Discussion started: 22 April 2022


Atmospheric Chemistry and Physics Discussions

into the mechanism of SOA photodegradation during UV-irradiation, none of them directly measured photobleaching rates in the organic phase.

This study was prompted by a hypothesis that the mechanism of SOA photodegradation in dry and aqueous particle phases should be different. This was tested by UV-irradiation of toluene high-NO_x SOA directly on filters and in aqueous solution, and contrasting the reaction products and absorption spectra. Our second goal was to explore the importance of inorganic salts in photobleaching and photodegradation of aqueous SOA, and this was done by UV-irradiation of high-NO_x toluene SOA in a concentrated ammonium sulfate solution and pure water. We present high-resolution mass spectrometry and FTIR results to provide an analysis of changes in chemical composition during photodegradation in different conditions, as well as UV-Visible spectroscopy results to monitor decay of the overall absorbance by SOA. We find that the compositional changes differ significantly between the organic particle and aqueous photodegradation. The presence of 1 M aqueous ammonium sulfate does not appear to significantly impact the changes in SOA composition, but the photobleaching kinetics are modestly slowed under these conditions.

2 Methods

Experiments were performed at the University of California Irvine (UCI) and at the College of William and Mary (WM). A summary of the types of the experiments performed and datasets collected is provided in Table S1. Briefly, all SOA filter samples were prepared in the UCI smog chamber. Some filter samples were mailed to WM on dry ice for on-filter photodegradation experiments and infrared spectroscopy analysis. All aqueous phase photodegradation experiments, photobleaching kinetics measurements, and aerosol mass spectrometry experiments were carried out at UCI.

2.1 Secondary Organic Aerosol Generation

SOA was prepared in a ~5 m^3 Teflon chamber. The chamber was first humidified to 40% RH. Then H_2O_2 was injected through a heated inlet to achieve a mixing ratio of 2 ppm, followed by an injection of 1.5 ppm of toluene and 0.7 ppm of NO. UV-B lamps within the chamber with an emission spectrum centered at 310 nm were used to initiate photooxidation, with typical OH steady-state concentration of about 10^6 molecule cm^{-3}, similar to our previous work (Hinks et al., 2018). No seed particles were used. A Scanning Mobility Particle Sizer (TSI Model 3936), NO_y monitor (Thermo Scientific Model 42i-Y), and ozone monitor (Thermo Scientific Model 49i) were used during all experiments to track particle size distribution and NO, NO_y, and ozone mixing ratios. An Aerosol Mass Spectrometer (AMS) was also used in some experiments to observe aerosol composition during aerosol generation and collection. Particles were collected onto polytetrafluoroethylene (PTFE) filters (Millipore 0.2 μM pore size), then the filters were sealed and frozen at -20 ºC until the aging experiments were performed. Table 1 provides a summary of samples we ended up using in this work (it does not include additional samples prepared for preliminary tests to optimize the experimental conditions).

Table 1: Summary of samples prepared and the experiments they were used for at William and Mary (WM) and UC Irvine (UCI).

Filter Number (location)	Max SOA concentration (μg m^{-3})	Total SOA collected (mg)	Data sets collected[a]
1 (WM)	308	0.9	Online AMS, FTIR
2 (WM)	328	1.1	Online AMS, FTIR

https://doi.org/10.5194/acp-2022-278
Preprint. Discussion started: 22 April 2022

Atmospheric Chemistry and Physics Discussions

3 (UCI)	225	1.0	H_2O & Filter Offline AMS, ESI(+,-)
4 (UCI)	159	0.6	AS & H_2O kinetics, ESI(+,-)
5 (UCI)	178	0.8	AS & H_2O kinetics[b]
6 (UCI)	208	0.8	AS & H_2O kinetics[b]
7 (UCI)	126	0.8	Filter kinetics[b]
8 (UCI)	196	0.6	Filter kinetics[b]
9 (UCI)	156	0.7	Filter kinetics[b]

Footnote: [a]2 filters for FTIR experiments, 1 filter for splitting between aqueous and filter aging, 3 filters for splitting between aqueous and ammonium sulfate aging kinetics, and 3 filters for only filter aging kinetics. [b]AS & H_2O kinetics refers to kinetic experiments in 1 M ammonium sulfate and pure water solutions, while filter kinetics refers to kinetic experiments on the filter.

1.2 Aqueous Photodegradation

1.2.1 Aqueous Sample Preparation and Irradiation

Aqueous UV-irradiation of samples was carried out at UCI. After several preliminary experiments to determine the best combination of experimental parameters, including extraction methods and aging conditions, three filters of SOA (numbered 4, 5, 6 in Table 1) were collected. Each filter was cut in half so that half of the filter could be extracted and photolyzed in water and the other half extracted and photolyzed in 1 M ammonium sulfate. Each filter was weighed whole, and then a half of the filter was weighed for a more accurate estimation of the mass of aerosol used in each experiment. The SOA material was extracted from the filter half by shaking it gently for 10 min in 5 mL acetonitrile. The acetonitrile was then removed by rotary evaporation at room temperature (to avoid losing more volatile SOA compounds), and water or 1 M ammonium sulfate solution was added to the SOA residue for the photolysis experiments. The SOA mass concentration in the solutions was close to 250 μg mL^{-1} in all trials (the actual mass concentrations for individual trails are shown in Table S2), and the unadjusted pH of the solutions was about 4.5 in both the ammonium sulfate and pure water conditions. These values are comparable to atmospheric cloud water, which generally contains about 200 μg mL^{-1} of dissolved organics and has pH values of between 3 and 6 (Collett et al., 2002, 2008; Herrmann et al., 2015). The solutions were split into three 0.7 to 1 mL (depending on the mass of SOA on the filter) aliquots to serve as the unaged, dark aged, and photolyzed samples. The aliquot designated as "unaged" was prepared immediately before the mass spectrometry analysis as described in the next paragraph. The photolyzed sample was exposed to near-UV radiation from a Xenon arc lamp (Newport Model 66902). The broadband light was reflected at a 90^0 angle with a dichroic mirror, and then passed through a 295 nm long-pass filter (Schott WG295) and a UV bandpass filter (Schott BG1) to remove UVC and visible wavelengths, leaving the majority of the radiation between 280 and 400 nm. A comparison of our lamp spectrum and ambient sunlight is shown in Fig. S1 and Table S3. The comparison shows that, in terms of the 280-400 nm radiation dose, 1 h in our photolysis set up is equivalent to approximately 1.7 h under the 24-hour average Los Angeles solar flux (average taken for June 20^{th}) as calculated using the Quick TUV calculator (ACOM: Quick TUV, 2019). Photolysis was carried out for 5 h through a 0.5 cm quartz cuvette containing SOA solution exposed to open air.

As high concentrations of inorganic ions should not be used with electrospray mass spectrometry, it was necessary to remove the ammonium sulfate from the SOA solutions before performing mass spectrometry analysis. To accomplish this, the majority of the water was removed by rotary evaporation at room temperature. Solvent removal was stopped when the ammonium sulfate began to precipitate out of solution, but care was taken to not evaporate to dryness, as evaporation of water in the presence of

https://doi.org/10.5194/acp-2022-278
Preprint. Discussion started: 22 April 2022


Atmospheric Chemistry and Physics Discussions

ammonium sulfate has been shown to cause condensation-type reactions that change the SOA composition (Nguyen et al., 2012). The SOA was extracted from the vial containing ammonium sulfate with 5 mL of acetonitrile in two 2.5 mL rinses. This acetonitrile was also removed by rotary evaporation at room temperature, and a 1:1 mixture of water:acetonitrile was added to the SOA such that the SOA concentration was about 350 μg mL^{-1}, assuming complete extraction, for mass spectrometry analysis. The same procedure was used for the solutions which did not contain ammonium sulfate for the sake of consistency.

2.2.2 UV-Vis Spectroscopy

A UV-Vis spectrometer (Shimadzu UV-2450) was used to observe the change in optical properties with photolysis in water or 1 M ammonium sulfate solution. The UV-Vis data were used to calculate the mass absorption coefficient (MAC):

$$MAC(\lambda) = \frac{A_{10}(\lambda)\times \ln(10)}{b\times C_{org}} \quad (1)$$

where $A_{10}(\lambda)$ is base-10 absorbance, b is the path length, and C_{org} is the mass concentration of the SOA sample in solution (g mL^{-1}). Additionally, SOA recovery for each step of the procedure was roughly determined by UV-Vis spectroscopy as the experiment went on, and the results of these checks are shown in Fig. S2. After the initial extraction of the filter with 5 mL of acetonitrile, the filter was re-extracted in 3 mL of methanol and a UV-Vis spectrum was taken, showing the SOA extraction efficiency by acetonitrile from the filter was 90% or greater (the first UV-Vis spectrum was taken while the SOA was dissolved in 3 mL of water, so this should be an approximately equivalent comparison). SOA recovery from the ammonium sulfate solution was also tested. After the SOA was extracted from the evaporated solution of SOA in ammonium sulfate, 1 mL of water was added back to the residual salt, replacing the 1 mL of water which had been removed by rotary evaporation, and a UV-Vis spectrum was taken. Comparison of the post-extraction spectrum with the initial spectrum show that the extraction procedure generally recovered about 50-70% of the SOA from the ammonium sulfate solution. Results of a similar procedure with the samples which did not contain ammonium sulfate showed that more than 90% of the SOA was extracted if ammonium sulfate was not present. The reason for the retention of some 30-50% SOA by the wet ammonium sulfate residue is unclear, and will be investigated in the future.

2.2.3 UPLC-PDA-HRMS

Changes in the molecular composition of the UV-irradiated SOA were analyzed by high-resolution mass spectrometry (HRMS) similar to as described previously (Chin et al., 2021). Briefly, the instrument was a Thermo Q-Exactive Plus mass spectrometer with a resolving power of 1.4×10^5 at *m/z* 400 equipped with a heated electrospray ionization inlet. The instrument was operated in both positive (spray voltage +3.5 kV) and negative ion mode (spray voltage -2.5 kV). Ultrahigh performance liquid chromatography (UPLC) and photodiode array (PDA) detection (scanning 190 to 680 nm) were performed to analyze the relative contribution of individual compounds to the total SOA absorption. The column was Phenomenex Luna Omega Polar C18, 150 × 2.1 mm, with 1.6 μm particles and 100 Å pores. The UPLC solvent gradient was 95% solvent A (water acidified to pH 3 with 0.1% formic acid) and 5% solvent B (acetonitrile acidified with 0.1% formic acid) for minutes 0 to 3, followed by a linear ramp to 95% solvent B and 5% solvent A from 3 to 14 minutes, a hold at 95% solvent B from 14 to 16 minutes, and a linear ramp back to 95% solvent A and 5% solvent B for 16 to 22 minutes in preparation for the next run. Separating the samples via liquid chromatography provided the benefit of reducing matrix effects and preventing ionization suppression from any inorganic ions not removed during the extraction process.

https://doi.org/10.5194/acp-2022-278
Preprint. Discussion started: 22 April 2022


Atmospheric Chemistry and Physics Discussions

Analysis of the PDA-HRMS data was performed using FreeStyle 1.6 from Thermo Scientific, and the peaks with the greatest integrated absorbance between 340 and 360 nm were correlated to the peaks in the total ion chromatogram (TIC) based on the instrument's PDA-MS time delay of 0.06 min. Molecular formulas for these chromophores were determined using FreeStyle. Additionally, FreeStyle was used to integrate over the full total ion chromatogram and generate a raw time-integrated (1 to 18 min) mass spectrum. Decon2LS (https://omics.pnl.gov/software/decontools-decon2ls) was used to extract peak positions and relative intensities from the time-integrated mass spectrum, and peaks representing ^{13}C compounds were removed. Peaks from the solvent, unaged, and two aging conditions were aligned with a tolerance of 0.0005 *m/z*. Peaks that were present in the solvent at the same or greater intensity as the samples were also removed. Finally, the mass spectra were assigned assuming an accuracy of 0.0005 *m/z* with a formula of $[C_cH_hO_xN_{0-3}S_{0-1} + Na]^+$ and $[C_cH_hO_xN_{0-3}S_{0-1} + H]^+$ for positive ion mode and $[C_cH_hO_xN_{0-3}S_{0-1} - H]^-$ for negative ion mode (although no sulfur-containing compounds were identified with greater than 0.01% abundance of the maximum peak height). Assigned peaks were used to verify the internal calibration of the *m/z* axis in both ion modes and adjust the calibration if needed. The internal calibration improved the *m/z* accuracy and usually led to a few additional assignments for peaks that could not be assigned within 0.0005 *m/z* in the uncalibrated mass spectra. Finally, neutral formulas were determined from the assignments, and the data from the positive and negative ion modes were clustered together. The mass spectra presented below show the combined peak abundance in the positive and negative ion mode data referenced to formulas of the unionized SOA compounds.

2.3 On-filter Photolysis

2.3.1 Sample Preparation and Irradiation

Preliminary on-filter photolysis experiments were performed at WM (experimental details are described in the SI section) and then replicated at UCI to allow better intercomparison with the aqueous results using the same photolysis set-up. Both photobleaching kinetics and UPLC-PDA-HRMS experiments for the on-filter samples were performed at UCI. Filters were cut into quarters, and each quarter was weighed to get a better estimate of the mass of toluene SOA used for each data point. For aging, one filter quarter was placed in front of the photolysis setup described in the aqueous photolysis section above such that the filter surface was uncovered and open to laboratory air. While not being photolyzed, the other filter quarters were re-sealed and kept frozen. After photolysis, the filter quarter was extracted with acetonitrile to take a UV-Vis spectrum with the instrument described above. Since UV-Vis sample preparation was destructive, each time point required an entire filter quarter and so only four time points could be taken per filter. Based on the observed photobleaching rate, 0, 1, 3, and 5 h were chosen as time points.

2.3.2 Aerosol Mass Spectrometry

A High-Resolution Time-of-Flight Aerosol Mass Spectrometer (HR-ToF-AMS or AMS; Aerodyne, Billerica, MA, USA) operated online in V-mode was used to monitor the SOA composition during SOA formation. Particles were vaporized at 600 °C and ionized using electron impact ionization at 70 eV. Additionally the AMS was used to analyze the composition during and after photolysis using a custom ultrasonic small volume nebulizer as described elsewhere (O'Brien et al., 2019). Briefly, sample preparation involved combining ~3 µL of sample solutions with ~2 µL of internal standard solution, consisting of a mixture of 0.25 g L^{-1} isotopically labelled $NH_4{}^{15}NO_3$ and 0.25 g L^{-1} NH_4I. The 5 µL of prepared sample were then loaded onto a clean Kapton film in the nebulizer. The sample was nebulized and the aerosol particles were carried with a flow of clean air into the inlet of the AMS. The AMS data were analyzed using ToF-AMS Analysis Toolkit 1.63H and ToF-AMS HR Analysis 1.23H.

https://doi.org/10.5194/acp-2022-278
Preprint. Discussion started: 22 April 2022

Atmospheric Chemistry and Physics Discussions

The signals for the NO^+ and NO_2^+ ions were quantified for each injection and intercompared between different samples after calculating the ratios with the signals for the corresponding isotopically labelled ions from the ammonium nitrate internal standard ($^{15}NO^+$ and $^{15}NO_2^+$).

3 Results and Discussion

3.1 Optical Properties

Figure 1 shows how the wavelength-dependent mass absorption coefficient of toluene SOA changes with photolysis in water. Mass absorption coefficient data for the other photolysis and dark conditions are provided in Fig. S3. The decrease in the absorption band at 350 nm over the five hours of photolysis was used to calculate the photobleaching lifetime of the chromophoric compounds in SOA. Previous work on toluene SOA suggests this absorption is mostly attributable to the π to π^* transition of nitrophenols, such as methylnitrocatechol (Lin et al., 2015).

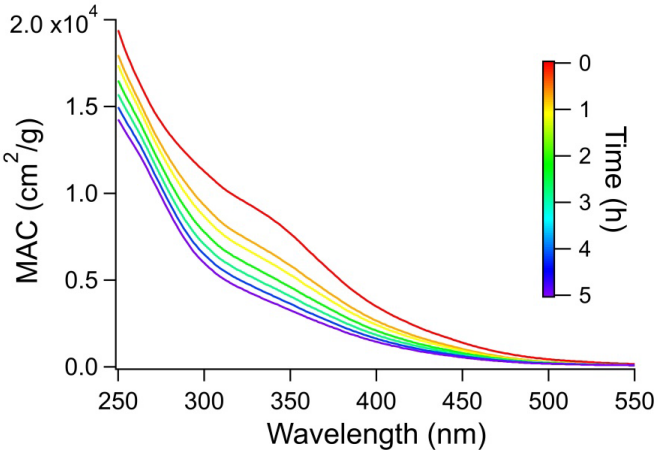

Figure 1: Representative wavelength-dependent mass absorption coefficient (MAC) values recorded during photolysis of toluene SOA. This figure shows aging in pure water, but MAC plots for other conditions are qualitatively similar. Absorption band at 350 nm decreases with 5 h of photolysis.

The time-dependent change in absorbance at 350 nm for all photolysis conditions is shown in Fig. 2. The absorbances over time were normalized to the initial absorbance and then were fit to the biexponential decay shown in equation (2),

$$y(t) = y_0 + A_1 e^{-k_1 t} + A_2 e^{-k_2 t} \quad (2)$$

where $y(t)$ is the absorbance as a function of time, y_0 represents photorecalcitrant fraction of the absorbance, k_1 and k_2 are rate constants for a faster and slower process, and A_1 and A_2 are relative absorbance contributions of compounds decaying through the faster and slower processes, respectively. We stress that this is a purely empirical fit, as in reality there are a large number of light-absorbing compounds in SOA, each with its own complex time dependence.

In the case of the aqueous samples, photolysis of one sample was continued for up to 24 h, after which most absorbance had decayed (Fig. S4). Since this suggests no significant photorecalcitrant fraction for these samples, y_0 could be set to zero for the water and 1 M ammonium sulfate aging conditions. However, both the faster and slower processes had to be included in order to adequately fit the data. In contrast, photolysis was much slower on the filter, and only one decay constant could be reliably

https://doi.org/10.5194/acp-2022-278
Preprint. Discussion started: 22 April 2022

Atmospheric Chemistry and Physics Discussions

determined from the data. Therefore, A_2 was constrained to zero for these samples to avoid over-fitting, but y_0 was included as a fit parameter. Previous studies have found significant fraction of photorecalcitrant material when SOA photolysis was performed in the organic particle phase (O'Brien and Kroll, 2019; Walhout et al., 2019; Baboomian et al., 2020; Pospisilova et al., 2021), so it is reasonable to have a non-zero y_0 for the on-filter photolysis condition. Future longer-term photolysis experiments on filters can help quantify what fraction of the material is fully photorecalcitrant in the atmosphere versus much slower than the rates observed for the aqueous samples.

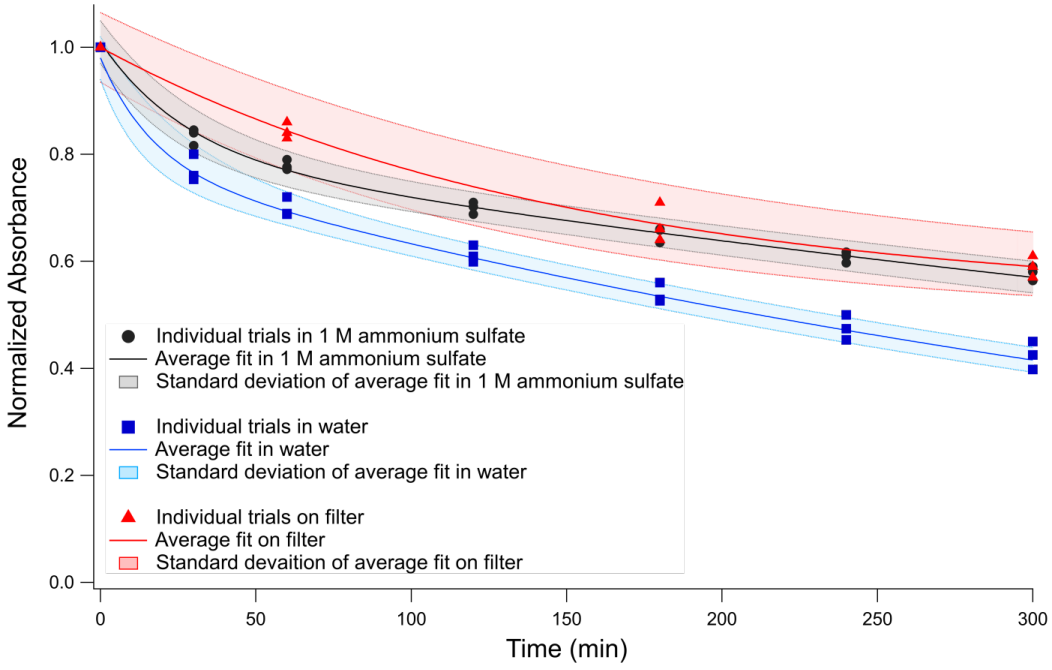

Figure 2: Normalized absorbance decay at 350 nm with photolysis. Photolysis experiments in 1 M ammonium sulfate are shown in black circles, in pure water are shown in blue squares, and on the filter are shown in red triangles. Values on the y-axis are normalized to the mass absorption coefficient at zero minutes. Shaded areas represent one standard deviation of the fit of the three combined trials.

Calculated fitting parameters from Fig. 2 are shown in Fig. S5 and summarized in Table S4. Absorbance lifetimes calculated from these values are shown in Table 2. The shortest photobleaching lifetimes are seen for photolysis in water, while the lifetimes are about twice as long in 1 M ammonium sulfate. An important result of this work is that SOA irradiation on the filter results in photobleaching that is nearly an order of magnitude slower than in pure water and a large photorecalcitrant absorbance fraction (53 ± 3%) is estimated. It should be noted that this fraction of the photorecalcitrant absorbance is similar to Baboomian et al. (2020) estimate of 50% photorecalcitrant mass fraction after photolysis of toluene-derived high-NO_x SOA deposited on a gold surface.

Table 2: Absorbance lifetimes and photorecalcitrant fractions for photobleaching processes described by Eq (2) scaled to the 24-h average solar actinic flux in Los Angeles. The unscaled measured rate constants are provided in Table S4. Errors represent the standard deviations over the three combined trials.

https://doi.org/10.5194/acp-2022-278
Preprint. Discussion started: 22 April 2022

Atmospheric Chemistry and Physics Discussions

	τ_1 (h)	τ_2 (h)	y_0
H_2O	0.5 ± 0.2	13.5 ± 0.6	NA
1 M ammonium sulfate	0.8 ± 0.1	25 ± 2	NA
Filter	4.0 ± 0.6	NA	0.53 ± 0.03

3.2 Chemical Composition Changes with Photolysis

3.2.1 PDA Data

In an effort to tie the photobleaching behavior observed in the UV-Vis data to changes in composition, UPLC-PDA-HRMS was performed on the samples before and after aging. PDA data for the photolysis conditions are shown in Fig. 3 – unaged, photolyzed in water, and photolyzed on filter from Filter 3 (Fig. 3a) and unaged, photolyzed in water, and photolyzed in 1 M ammonium sulfate from Filter 4 (Fig. 3b). Because the fastest absorbance decrease with photolysis was observed at 350 nm, the PDA counts were integrated from 340 to 360 nm to focus on this feature. A large fraction of the eluting compounds were unresolved, forming a very broad peak stretching from 5 to 12 min. Superimposed on top of the unresolved peaks were several well-resolved peaks. In the unaged chromatogram, the most abundant species corresponding to major PDA peaks are all nitrophenol type compounds – $C_7H_7NO_3$ (nitrocresol - 10.36 min), $C_7H_7NO_4$ (three structural isomers of methylnitrocatechol - 8.04, 9.14, and 9.69 min), and $C_6H_5NO_3$ (nitrophenol - 9.35 min). These are also the most abundant compounds in the integrated mass spectrum shown in Fig. 4(a).

https://doi.org/10.5194/acp-2022-278
Preprint. Discussion started: 22 April 2022

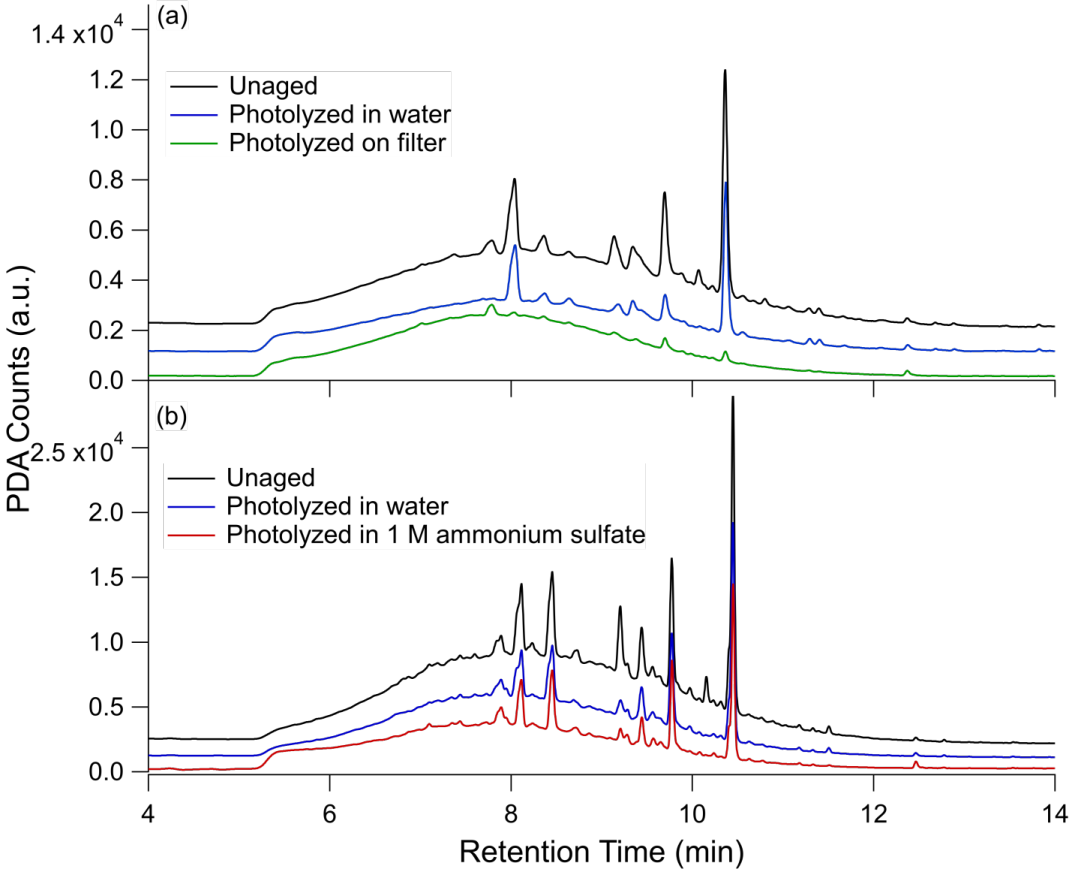

Figure 3: UPLC-PDA chromatograms for a.) unaged toluene SOA sample (black trace), photolyzed 5 h in water (blue trace), and photolyzed 5 h on the filter (green trace) and b.) unaged toluene SOA (black trace), photolyzed 5 h in water (blue trace), and photolyzed 5 h in 1 M ammonium sulfate (red trace). PDA counts were integrated over 340 to 360 nm wavelength range to emphasize the UV-Vis feature at 350 nm which decays with photolysis. In the case of 1 M ammonium sulfate, PDA counts were adjusted for the estimated 50% extraction efficiency, causing some variation in the baseline. Additionally, the baselines are each offset by 10^3 PDA counts on the y-axis for ease of comparison.

In Fig. 3(a), a significant difference can be seen in the PDA data after photolysis on the filter compared to photolysis in water. After five hours of photolysis in water (blue trace) there is not much change in the resolved features, but after five hours of photolysis on the filter (green trace) the resolved features are greatly reduced. By contrast, the height of the unresolved absorbance in the filter photolysis looks similar to the unaged sample (black trace) while the unresolved absorbance in the aqueous photolysis trace appears to have decreased somewhat in intensity. The control conditions, shown in Fig. S6, show no obvious change in resolved or unresolved peak shape with dark aging.

Figure 3(b) compares the PDA absorbance with photolysis in water and 1 M ammonium sulfate. The addition of ammonium sulfate does not appear to have changed the shape of the PDA chromatogram to a large degree, although the lower extraction efficiency may influence these results. If some compounds preferentially remain with the ammonium sulfate after extraction, we will miss them in this analysis.

https://doi.org/10.5194/acp-2022-278
Preprint. Discussion started: 22 April 2022


Atmospheric Chemistry and Physics Discussions

3.2.2 SOA Composition – High Resolution Mass Spectrometry

Unaged toluene SOA composition has been well characterized using HRMS previously (Lin et al., 2015), so we will focus our discussion on composition changes before and after photolysis. Figure 4 compares the time-integrated SOA mass spectra for photolysis in water and on filter, while Fig. 5 contrasts the behavior of SOA from a separate experiment in water and in 1 M ammonium sulfate. In all cases, the mass spectra represent combined positive and negative ion mode mass spectra scaled to the approximate mass concentration of organics in the samples. The mass spectra, including the sample aged with 1 M ammonium sulfate in Fig. 5(c), show excellent reproducibility after accounting for the concentration of organics in the mass spectrometry samples, demonstrating that the extraction method used here is effective for extracting SOA samples for mass spectrometry analysis. The unaged SOA mass spectra are dominated by nitrogen-containing compounds, the most abundant of which are $C_7H_7NO_3$ (153 Da) and $C_7H_7NO_4$ (169 Da), in agreement with previous work on high-NOx toluene SOA (Jang and Kamens, 2001; Lin et al., 2015; Hinks et al., 2018).

A comparison of mass spectra in Fig. 4(a) (unaged) and 4(b) (photolyzed in water) suggests that photolysis in water does not lead to a large change in the overall composition. There is some decrease in the abundance of nitrogen-containing compounds upon UV-irradiation, but many of the major peaks are the same as in the unaged spectrum. Some formation of CHO compounds at lower molecular weights (less than 150 Da) can be seen. These are not observed in the dark-aged aqueous samples (see Fig. S7 and Fig. S8). The peaks that are most different in abundance between the photolysis and dark samples (such that they are among the 10 most abundant peaks after photolysis but not after dark aging) are present at much greater abundances in the negative mode than the positive mode, and can be assigned to small organic acids, such as maleic acid at 116 Da. Organic acids are established aqueous photolysis products of nitrophenols (Alif et al., 1991).

The difference in the composition after on-filter photolysis (Fig. 4(c)) is much more apparent. In contrast to the aqueous photolysis condition (Fig. 4(b)) where the nitrogen-containing peaks are relatively unaffected, the nitrogen-containing peaks in the organic-rich phase are greatly reduced in abundance with photolysis – such that the peak abundance of CHON compounds is less than that of CHO. The CHO compound abundance appears relatively unchanged. We do not observe an increase in peak abundances at low molecular weights as we did with aqueous photolysis. This suggests the photolysis products may be different in the organic phase as compared to the aqueous phase. We should note that the aqueous photolysis products may remain dissolved in water after formation, while those from filter photolysis may escape into the gas phase if they are formed on the surface of the SOA film.

https://doi.org/10.5194/acp-2022-278
Preprint. Discussion started: 22 April 2022

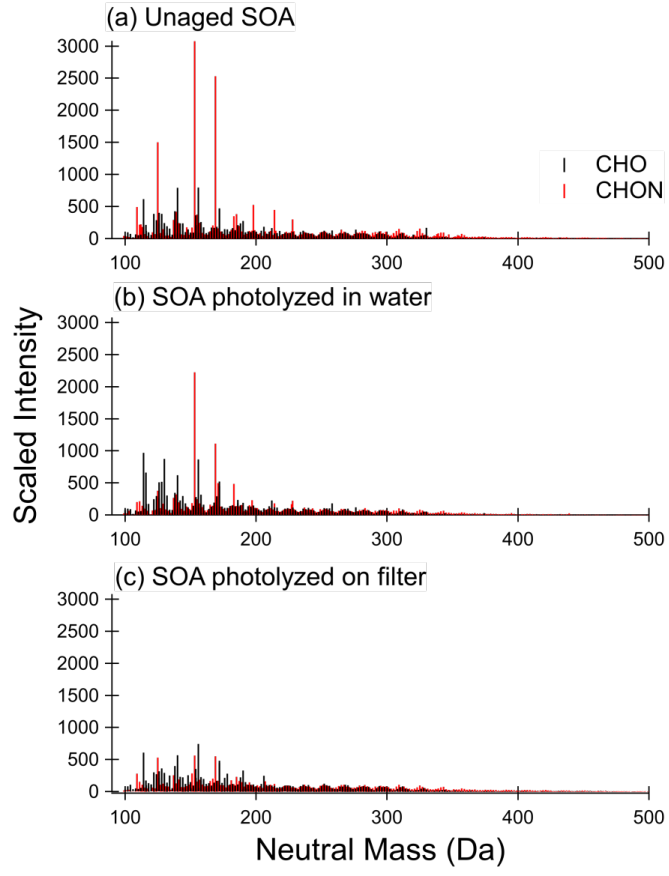

Figure 4: Mass spectra for (a) unaged SOA sample, (b) SOA sample photolyzed 5 h in water, and (c) SOA sample photolyzed 5 h on the filter. CHON compounds are shown in red and CHO compounds are shown in black. The signal is scaled to approximate pre-photolysis mass concentration of SOA in mass spectrometry samples. Control (dark aged) samples are shown in Fig. S7.

The results of aging in water appear reproducible when comparing the top two panels of Fig. 4 and 5 – little change is observed other than a modest increase in abundance of low molecular weight CHO compounds. Further, the addition of 1 M ammonium sulfate (Fig. 5(c)) did not have a significant impact on the composition after photolysis as compared to pure water (Fig. 5(b)). There does seem to be less increase in low molecular weight CHO compounds, which is reasonable considering the photobleaching was about half as fast in the ammonium sulfate condition as the pure water condition. We conclude that ammonium sulfate did not have a large effect on changes in SOA composition with photolysis as compared to pure water, but rather simply slowed down the photolysis rate.

https://doi.org/10.5194/acp-2022-278
Preprint. Discussion started: 22 April 2022

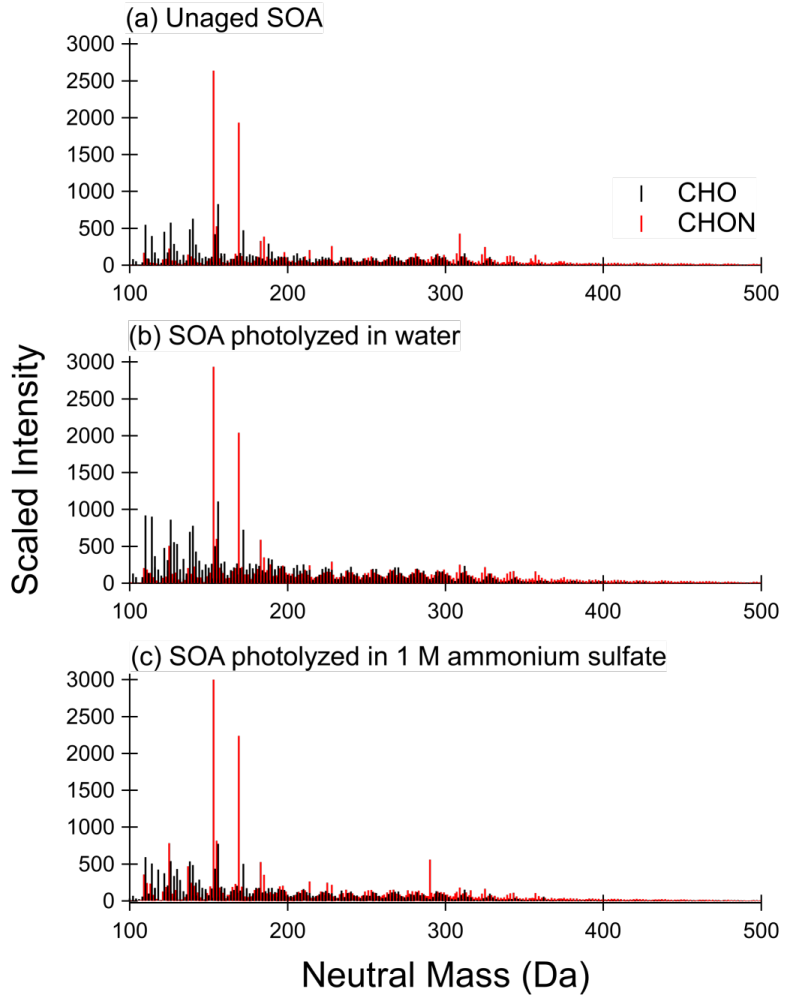

Figure 5. Mass spectra for (a) unaged SOA sample, (b) SOA sample photolyzed 5 h in water, and (c) SOA sample photolyzed 5 h in 1 M ammonium sulfate. CHON compounds are shown in red and CHO compounds are shown in black. Signal is scaled to approximate pre-photolysis mass concentration of SOA in mass spectrometry samples. Control (dark aged) samples are shown in Fig. S8.

3.2.3 Changes in Nitrogen-Containing Groups with Photolysis on Filters

To confirm removal of nitrogen-containing compounds with on-filter photolysis, nitrogen content was quantified from offline-AMS data by normalizing the NO^+ and NO_2^+ signal to the labelled NO^+ and NO_2^+ signals from the internal standard as shown in Fig. 6. The normalization accounts for variations in the signal for each nebulization pulse, which has been demonstrated to occur with the small volume nebulizer (O'Brien et al., 2019). Organonitrates and organic nitro groups generate NO^+ and NO_2^+ when ionized in the AMS, thus differences in the total amount of these ions suggests a loss of these functional groups in the samples (Farmer et al., 2010). Before photolysis, the nitrogen-containing moiety concentration for the aqueous and filter samples is slightly outside of each other's standard deviation, which may be a result of composition differences while the AMS samples are

https://doi.org/10.5194/acp-2022-278
Preprint. Discussion started: 22 April 2022

Atmospheric Chemistry and Physics Discussions

being formed or a small variation in extraction efficiencies between the two filter halves. After aging there is no apparent change in nitrogen content after five hours of photolysis in pure water. In stark contrast, there is a reduction in nitrogen content after five hours of photolysis directly on the filter. FTIR data, shown in Fig. S9, also fully support the loss of nitrogen-containing groups with on-filter photolysis. Peaks corresponding to both organonitrates and nitroaromatics decreased over time with photolysis relative to carbonyl peaks (more details are provided in the SI). Both the AMS and the FTIR results agree well with the relatively qualitative ESI results.

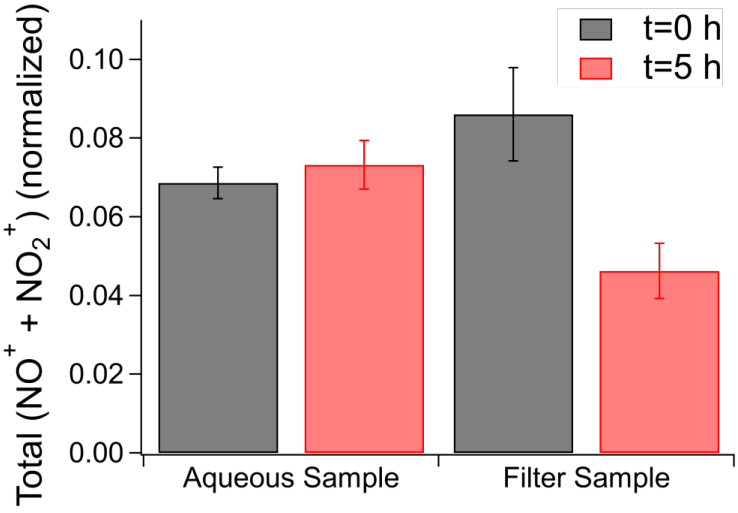

Figure 6. Totals for the main fragment ions for nitrogen-containing groups measured by aerosol mass spectrometry before (in black) and after 5 h of photolysis (in red) in the aqueous phase and organic particle phase. NO^+ and NO_2^+ fragment concentrations are normalized to an internal standard. Error bars represent one standard deviation over five injections.

3.2.4 Effect of Photolysis Matrix on Photo-degradation Mechanism

It is clear from the composition data that the photolysis of toluene SOA proceeds differently in the viscous organic phase compared to the aqueous phase. Our experiments show that nitrophenols, which are mostly resolved in the PDA data and are expected to be major chromophores in this SOA, are preferentially photolyzed in the viscous organic phase. Previous studies have established that nitrophenols photolyze more quickly in the organic phase than in the aqueous phase, and the proposed mechanism is abstraction of a hydrogen atom from surrounding organic molecules by a triplet state of an excited nitrophenol (Lignell et al., 2014a; Dalton and Nizkorodov, 2021). For 3-nitropyrene, hydrogen abstraction was observed to be nearly diffusion controlled, while charge transfer reactions were not observed in organic solvents (Scheerer and Henglein, 1977). Further, it was observed for nitro-polycyclic aromatic hydrocarbons (PAH) that phenolic hydrogens were most efficiently abstracted by the triplet excited states, with other types of easily-abstractable hydrogens not participating in photodegradation (Feilberg and Nielsen, 2000). We expect a significant fraction of phenolic compounds in our SOA, and in the organic phase an excited triplet state will be in closer proximity to abstractable phenolic hydrogens than in the aqueous phase, making this a plausible explanation for relatively fast removal of CHON compounds in the organic phase. Additionally, oxy-PAHs with an n to π^* triplet character have been shown to strongly accelerate nitro-PAH decay through the initiation of a radical chain reaction (Feilberg and Nielsen, 2000). This pathway is more important in the organic phase than in the aqueous phase because differences

https://doi.org/10.5194/acp-2022-278
Preprint. Discussion started: 22 April 2022


Atmospheric Chemistry and Physics Discussions

in matrix polarity change the relative energies of the n to π^* and π to π^* transitions for many aromatic carbonyls, such that the more reactive n to π^* transition is favored in less polar matrices and the less reactive π to π^* transition is favored in polar matrices (Horspool and Lenci, 2003). Combined, these mechanisms likely explain the relatively rapid loss of nitrophenols in the organic phase as observed by mass spectrometry.

In spite of *slower* photodegradation of nitrophenols in the aqueous phase, overall photobleaching was actually *faster* in the aqueous phase. Since we observed minimal composition change with mass spectrometry, photolysis in the aqueous phase must result in the decay of highly absorbing compounds with low abundance or poor electrospray ionization efficiency. This observation correlates well to Lin et al. (2015) observations, which catalogued the chromophores in toluene SOA, and attributed 40 to 60% of the PDA absorbance to poorly separated chromophores with low peak abundances in ESI mass spectra (Lin et al., 2015). Further, the fact that photobleaching is slowed with the addition of ammonium sulfate suggests that these lower abundance compounds may still react through a triplet state when photolyzed. Ionic species may quench an excited triplet compound before it reacts (Treinin and Hayon, 1976), leading to slower chromophore loss with the addition of ammonium sulfate. We therefore conclude that the triplet chemistry of brown carbon chromophores will strongly depend on the matrix during photolysis, with not only differing photobleaching rates, but very different composition changes occurring under different matrix conditions.

4 Conclusions/Atmospheric Implications

Toluene high-NO_x SOA was aged by direct photolysis on filters simulating the viscous organic phase in aerosol particles and in aqueous solution with and without 1 M ammonium sulfate representing dilute atmospheric cloud water and concentrated aerosol-phase water, respectively. UV-Vis measurements reported here show that photobleaching is fastest in pure water, while the presence of ammonium sulfate modestly slows the rates of photobleaching. Photobleaching in the viscous organic phase is much slower and a large fraction of photorecalcitrant absorbance is observed. Chromatographic analysis showed that nitrophenols as well as a large number of unresolved chromophores contribute to the absorption coefficient by SOA. We find that the decay of nitrophenol compounds proceeds much more quickly in the viscous organic phase than in the aqueous phase, in agreement with previous studies measuring the photolysis of single nitrophenols in aqueous solutions and viscous organics (Dalton and Nizkorodov, 2021). In contrast, the SOA composition of the aqueous phase samples does not change appreciably over the 5 h photolysis experiment in spite of the observed faster photobleaching. This suggests preferential photodegradation of unidentified chromophores with low peak abundance in the mass spectra but high absorptivity.

We ascribe the differences in photolytic aging to differences in triplet state reactivity between sample matrices. Previous work has observed different photolysis rates for the same chromophore in different atmospherically-relevant environments, such as water, alcohol solutions, and glassy organic matrices (Fleming et al., 2020; Dalton and Nizkorodov, 2021; Hinks et al., 2016; Lignell et al., 2014b). These studies mostly focused on the photolysis of select nitrophenol compounds, and found nitrophenols to photolyze faster in the organic solvents than in water. Our results confirm that SOA nitrophenols, as a group, appear to the more efficiently photolyzed chromophores in the organic phase. However, this cannot be generalized to all chromophores because we observe that other, presently unidentified, chromophores are more efficiently photolyzed in aqueous solution. Therefore, generally speaking, photolysis rates of individual major chromophores can be quite different from the overall photobleaching rates, particularly when measured in the aqueous phase, and the study of individual chromophores does not fully represent the behavior of complex SOA particles.

https://doi.org/10.5194/acp-2022-278
Preprint. Discussion started: 22 April 2022


Atmospheric Chemistry and Physics Discussions

Reaction with the OH radical is considered the most important photochemical sink for organic molecules in the atmosphere. In the case of SOA, biomass burning organic aerosol, and individual nitrophenol compounds, OH reactions are often observed to cause chromophore formation for a short time period before leading to photobleaching for both heterogeneous reactions on particles and reactions in the aqueous phase (Hems et al., 2021). Subsequent photobleaching of various BrC aerosol types have a wide variety of OH lifetimes ranging from hours to days, which is on the same order we measure for our UV-irradiation experiments (Hems et al., 2021). Nitrophenols react relatively quickly with OH in the aqueous phase – lifetimes of several hours have been reported for a few representative compounds – so OH will likely be a more important sink for nitrophenols in clouds and aqueous aerosol (Zhao et al., 2015; Hems and Abbatt, 2018). However, since we observe that photobleaching occurs much more quickly than nitrophenol loss in the aqueous phase, we can expect both OH reaction and photodegradation to be important factors affecting the lifetimes with respect to photobleaching and lifetimes of individual chromophores in the atmosphere.

The results reported here will likely vary depending on ionic strength or particle viscosity. The ammonium sulfate concentration used here – 1 M – is on the low end of ionic strengths found in atmospheric particles (Herrmann et al., 2015). Higher salt concentrations will likely quench triplet reactivity more efficiently and so may slow photodegradation further. Future work is needed to determine the precise relationship between the ionic strength and photobleaching rate for different types of SOA. Furthermore, this study was limited to ammonium sulfate, but other anions, such as halides, are more effective triplet quenchers than sulfate (Jammoul et al., 2009; Gemayel et al., 2021). More importantly, more work on the impact of the matrix viscosity on photodegradation of SOA should be done. Previous studies have found higher viscosity to both slow and accelerate photodegradation of individual nitroaromatics (Hinks et al., 2016; Dalton and Nizkorodov, 2021). The conflicting results are likely due to the reactivity of nearby molecules during photolysis as well as triplet lifetime of the absorber. Therefore, it will be useful to independently vary the organic matrix viscosity and the types of surrounding species in future studies in order to fully understand the factors controlling photobleaching and photodegradation lifetimes of SOA.

Acknowledgements

The UCI team acknowledges support from NSF grant AGS-1853639, and thanks Natalie R. Smith for helping take UPLC-PDA-HRMS data during the pandemic time. The WM team acknowledges support from NSF grant AGS-2042619 and William & Mary Honors research funding. The WM team also thanks William McNamara for the use of the arc lamp. The authors thank NSF grant AGS-1936123 for covering the open access publication fees.

References

ACOM: Quick TUV: http://cprm.acom.ucar.edu/Models/TUV/Interactive_TUV/, last access: 11 July 2019.

Alif, A., Pilichowski, J. F., and Boule, P.: Photochemistry and environment XIII: Phototransformation of 2-nitrophenol in aqueous solution, J. Photochem. Photobiol. A Chem., 59, 209–219, https://doi.org/10.1016/1010-6030(91)87009-K, 1991.

Baboomian, V. J., Gu, Y., and Nizkorodov, S. A.: Photodegradation of secondary organic aerosols by long-term exposure to solar actinic radiation, ACS Earth Sp. Chem, 4, 1078–1089, https://doi.org/10.1021/acsearthspacechem.0c00088, 2020.

Badali, K. M., Zhou, S., Aljawhary, D., Antiñolo, M., Chen, W. J., Lok, A., Mungall, E., Wong, J. P. S., Zhao, R., and Abbatt, J. P. D.: Formation of hydroxyl radicals from photolysis of secondary organic aerosol material, Atmos. Chem. Phys., 15, 7831–7840, https://doi.org/10.5194/ACP-15-7831-2015, 2015.

Bikkina, S., Kawamura, K., and Sarin, M.: Secondary organic aerosol formation over coastal ocean: Inferences from atmospheric water-soluble low molecular weight organic compounds, Environ. Sci. Technol., 51, 4347–4357,

https://doi.org/10.1021/acs.est.6b05986, 2017.

Chin, H., Hopstock, K. S., Fleming, L. T., Nizkorodov, S. A., and Al-Abadleh, H. A.: Effect of aromatic ring substituents on the ability of catechol to produce brown carbon in iron(III)-catalyzed reactions, Environ. Sci. Atmos., 1, 64–78, https://doi.org/10.1039/D0EA00007H, 2021.

Collett, J. L., Bator, A., Sherman, D., Moore, K. F., Hoag, K. J., Demoz, B. B., Rao, X., and Reilly, J. E.: The chemical composition of fogs and intercepted clouds in the United States, Atmos. Res., 64, 29–40, https://doi.org/10.1016/S0169-8095(02)00077-7, 2002.

Collett, J. L., Herckes, P., Youngster, S., and Lee, T.: Processing of atmospheric organic matter by California radiation fogs, Atmos. Res., 87, 232–241, https://doi.org/10.1016/j.atmosres.2007.11.005, 2008.

Dalton, A. B. and Nizkorodov, S. A.: Photochemical Degradation of 4-Nitrocatechol and 2,4-Dinitrophenol in a Sugar-Glass Secondary Organic Aerosol Surrogate, Environ. Sci. Technol., 55, 14586–14594, https://doi.org/10.1021/ACS.EST.1C04975, 2021.

Epstein, S. A., Blair, S. L., and Nizkorodov, S. A.: Direct photolysis of α-pinene ozonolysis secondary organic aerosol: Effect on particle mass and peroxide content, Environ. Sci. Technol., 48, 11251–11258, https://doi.org/10.1021/es502350u, 2014.

Farmer, D. K., Matsunaga, A., Docherty, K. S., Surratt, J. D., Seinfeld, J. H., Ziemann, P. J., and Jimenez, J. L.: Response of an aerosol mass spectrometer to organonitrates and organosulfates and implications for atmospheric chemistry, Proc. Natl. Acad. Sci., 107, 6670–6675, https://doi.org/10.1073/pnas.0912340107, 2010.

Feilberg, A. and Nielsen, T.: Effect of Aerosol Chemical Composition on the Photodegradation of Nitro-polycyclic Aromatic Hydrocarbons, Environ. Sci. Technol., 34, 789–797, https://doi.org/10.1021/ES990566R, 2000.

Feng, Y., Ramanathan, V., and Kotamarthi, V. R.: Brown carbon: A significant atmospheric absorber of solar radiation, Atmos. Chem. Phys., 13, 8607–8621, https://doi.org/10.5194/acp-13-8607-2013, 2013.

Fleming, L. T., Lin, P., Roberts, J. M., Selimovic, V., Yokelson, R., Laskin, J., Laskin, A., and Nizkorodov, S. A.: Molecular composition and photochemical lifetimes of brown carbon chromophores in biomass burning organic aerosol, Atmos. Chem. Phys., 20, 1105–1129, https://doi.org/10.5194/ACP-20-1105-2020, 2020.

Gemayel, R., Emmelin, C., Perrier, S., Tomaz, S., Baboomian, V. J., Fishman, D. A., Nizkorodov, S. A., Dumas, S., and George, C.: Quenching of ketone triplet excited states by atmospheric halides, Environ. Sci. Atmos., 1, 31–44, https://doi.org/10.1039/D0EA00011F, 2021.

Hems, R. F. and Abbatt, J. P. D.: Aqueous phase photo-oxidation of brown carbon nitrophenols: Reaction kinetics, mechanism, and evolution of light absorption, ACS Earth Sp. Chem., 2, 225–234, https://doi.org/10.1021/acsearthspacechem.7b00123, 2018.

Hems, R. F., Schnitzler, E. G., Liu-Kang, C., Cappa, C. D., and Abbatt, J. P. D.: Aging of atmospheric brown carbon aerosol, https://doi.org/10.1021/acsearthspacechem.0c00346, 15 April 2021.

Henry, K. M. and Donahue, N. M.: Photochemical aging of α-pinene secondary organic aerosol: Effects of OH radical sources and photolysis, J. Phys. Chem. A, 116, 5932–5940, https://doi.org/10.1021/JP210288S, 2012.

Herrmann, H., Schaefer, T., Tilgner, A., Styler, S. A., Weller, C., Teich, M., and Otto, T.: Tropospheric aqueous-phase chemistry: Kinetics, mechanisms, and its coupling to a changing gas phase, Chem. Rev., 115, 4259–4334, https://doi.org/10.1021/cr500447k, 2015.

Hinks, M. L., Brady, M. V., Lignell, H., Song, M., Grayson, J. W., Bertram, A. K., Lin, P., Laskin, A., Laskin, J., and Nizkorodov, S. A.: Effect of viscosity on photodegradation rates in complex secondary organic aerosol materials, Phys. Chem. Chem. Phys., 18, 8785–8793, https://doi.org/10.1039/c5cp05226b, 2016.

Hinks, M. L., Montoya-Aguilera, J., Ellison, L., Lin, P., Laskin, A., Laskin, J., Shiraiwa, M., Dabdub, D., and Nizkorodov, S. A.:

480 Effect of relative humidity on the composition of secondary organic aerosol from the oxidation of toluene, Atmos. Chem. Phys., 18, 1643–1652, https://doi.org/10.5194/ACP-18-1643-2018, 2018.

Hodzic, A., Madronich, S., Kasibhatla, P. S., Tyndall, G., Aumont, B., Jimenez, J. L., Lee-Taylor, J., and Orlando, J.: Organic photolysis reactions in tropospheric aerosols: Effect on secondary organic aerosol formation and lifetime, Atmos. Chem. Phys., 15, 9253–9269, https://doi.org/10.5194/ACP-15-9253-2015, 2015.

485 Horspool, W. and Lenci, F. (Eds.): CRC Handbook of Organic Photochemistry and Photobiology, Volumes 1 & 2, Second Edi., CRC Press, 107-7-107-10 pp., https://doi.org/10.1201/9780203495902, 2003.

Hung, H. M., Chen, Y. Q., and Martin, S. T.: Reactive aging of films of secondary organic material studied by infrared spectroscopy, J. Phys. Chem. A, 117, 108–116, https://doi.org/10.1021/JP309470Z/SUPPL_FILE/JP309470Z_SI_001.PDF, 2013.

490 Jammoul, A., Dumas, S., D'Anna, B., and George, C.: Photoinduced oxidation of sea salt halides by aromatic ketones: A source of halogenated radicals, Atmos. Chem. Phys., 9, 4229–4237, https://doi.org/10.5194/ACP-9-4229-2009, 2009.

Jang, M. and Kamens, R. M.: Characterization of secondary aerosol from the photooxidation of toluene in the presence of NO_x and 1-propene, Environ. Sci. Technol., 35, 3626–3639, https://doi.org/10.1021/es010676+, 2001.

Ji, H., Lee, J., Aiona, P. K., Laskin, A., Laskin, J., and Nizkorodov, S. A.: Effect of solar radiation on the optical properties and

495 molecular composition of laboratory proxies of atmospheric brown carbon, Environ. Sci. Technol., 48, 10217–10226, https://doi.org/10.1021/es502515r, 2014.

Krapf, M., El Haddad, I., Bruns, E. A., Molteni, U., Daellenbach, K. R., Prévôt, A. S. H., Baltensperger, U., and Dommen, J.: Labile Peroxides in Secondary Organic Aerosol, 1, 603–616, https://doi.org/10.1016/J.CHEMPR.2016.09.007, 2016.

Laskin, A., Laskin, J., and Nizkorodov, S. A.: Chemistry of Atmospheric Brown Carbon, Chem. Rev., 115, 4335–4382,

500 https://doi.org/10.1021/cr5006167, 2015.

Lignell, H., Hinks, M. L., and Nizkorodov, S. A.: Exploring matrix effects on photochemistry of organic aerosols, Proc. Natl. Acad. Sci. U. S. A., 111, 13780–13785, https://doi.org/10.1073/PNAS.1322106111/SUPPL_FILE/PNAS.1322106111.SAPP.PDF, 2014a.

Lignell, H., Hinks, M. L., and Nizkorodov, S. A.: Exploring matrix effects on photochemistry of organic aerosols, Proc. Natl.

505 Acad. Sci. U. S. A., 111, 13780–13785, https://doi.org/10.1073/PNAS.1322106111/SUPPL_FILE/PNAS.1322106111.SAPP.PDF, 2014b.

Lin, P., Liu, J., Shilling, J. E., Kathmann, S. M., Laskin, J., and Laskin, A.: Molecular characterization of brown carbon (BrC) chromophores in secondary organic aerosol generated from photo-oxidation of toluene, Phys. Chem. Chem. Phys., 17, 23312–23325, https://doi.org/10.1039/C5CP02563J, 2015.

510 Liu, J., Lin, P., Laskin, A., Laskin, J., Kathmann, S. M., Wise, M., Caylor, R., Imholt, F., Selimovic, V., and Shilling, J. E.: Optical properties and aging of light-absorbing secondary organic aerosol, Atmos. Chem. Phys., 16, 12815–12827, https://doi.org/10.5194/acp-16-12815-2016, 2016.

Loisel, G., Mekic, M., Liu, S., Song, W., Jiang, B., Wang, Y., Deng, H., and Gligorovski, S.: Ionic strength effect on the formation of organonitrate compounds through photochemical degradation of vanillin in liquid water of aerosols, Atmos.

515 Environ., 246, 118140, https://doi.org/10.1016/j.atmosenv.2020.118140, 2021.

Luo, M., Shemesh, D., Sullivan, M. N., Alves, M. R., Song, M., Gerber, R. B., and Grassian, V. H.: Impact of pH and NaCl and CaCl2 salts on the speciation and photochemistry of pyruvic acid in the aqueous phase, J. Phys. Chem, 124, 5071–5080, https://doi.org/10.1021/acs.jpca.0c01016, 2020.

Malecha, K. T. and Nizkorodov, S. A.: Photodegradation of secondary organic aerosol particles as a source of small, oxygenated

volatile organic compounds, Environ. Sci. Technol., 50, 9990–9997, https://doi.org/10.1021/ACS.EST.6B02313, 2016.

Malecha, K. T., Cai, Z., and Nizkorodov, S. A.: Photodegradation of secondary organic aerosol material quantified with a quartz crystal microbalance, Environ. Sci. Technol. Lett., 5, 366–371, https://doi.org/10.1021/acs.estlett.8b00231, 2018.

Mang, S. A., Henricksen, D. K., Bateman, A. P., Andersen, M. P. S., Blake, D. R., and Nizkorodov, S. A.: Contribution of carbonyl photochemistry to aging of atmospheric secondary organic aerosol, J. Phys. Chemsitry A, 8337–8344, https://doi.org/10.1021/jp804376c, 2008.

Mekic, M., Brigante, M., Vione, D., and Gligorovski, S.: Exploring the ionic strength effects on the photochemical degradation of pyruvic acid in atmospheric deliquescent aerosol particles, Atmos. Environ., 185, 237–242, https://doi.org/10.1016/J.ATMOSENV.2018.05.016, 2018.

Nguyen, T. B., Lee, P. B., Updyke, K. M., Bones, D. L., Laskin, J., Laskin, A., and Nizkorodov, S. A.: Formation of nitrogen- and sulfur-containing light-absorbing compounds accelerated by evaporation of water from secondary organic aerosols, J. Geophys. Res. Atmos., 117, 1207, https://doi.org/10.1029/2011JD016944, 2012.

O'Brien, R. E. and Kroll, J. H.: Photolytic aging of secondary organic aerosol: Evidence for a substantial photo-recalcitrant fraction, J. Phys. Chem. Lett., 10, 4003–4009, https://doi.org/10.1021/ACS.JPCLETT.9B01417/SUPPL_FILE/JZ9B01417_SI_001.PDF, 2019.

O'Brien, R. E., Ridley, K. J., Canagaratna, M. R., Jayne, J. T., Croteau, P. L., Worsnop, D. R., Hapsari Budisulistiorini, S., Surratt, J. D., Follett, C. L., Repeta, D. J., and Kroll, J. H.: Ultrasonic nebulization for the elemental analysis of microgram-level samples with offline aerosol mass spectrometry, Atmos. Meas. Tech., 12, 1659–1671, https://doi.org/10.5194/AMT-12-1659-2019, 2019.

Pan, X., Underwood, J. S., Xing, J. H., Mang, S. A., and Nizkorodov, S. A.: Photodegradation of secondary organic aerosol generated from limonene oxidation by ozone studied with chemical ionization mass spectrometry, Atmos. Chem. Phys., 9, 3851–3865, https://doi.org/10.5194/ACP-9-3851-2009, 2009.

Pospisilova, V., Bell, D. M., Lamkaddam, H., Bertrand, A., Wang, L., Bhattu, D., Zhou, X., Dommen, J., Prevot, A. S. H., Baltensperger, U., El Haddad, I., and Slowik, J. G.: Photodegradation of α-pinene secondary organic aerosol dominated by moderately oxidized molecules, Environ. Sci. Technol., 55, 6936–6943, https://doi.org/10.1021/ACS.EST.0C06752/SUPPL_FILE/ES0C06752_SI_001.PDF, 2021.

Pruppacher, H. R. and Jaenicke, R.: The processing of water vapor and aerosols by atmospheric clouds, a global estimate, Atmos. Res., 38, 283–295, https://doi.org/10.1016/0169-8095(94)00098-X, 1995.

Ray, D., Ghosh, S. K., and Raha, S.: Impacts of some co-dissolved inorganics on in-cloud photochemistry of aqueous brown carbon, Atmos. Environ., 223, 117250, https://doi.org/10.1016/j.atmosenv.2019.117250, 2020.

Romonosky, D. E., Ali, N. N., Saiduddin, M. N., Wu, M., Lee, H. J. (Julie), Aiona, P. K., and Nizkorodov, S. A.: Effective absorption cross sections and photolysis rates of anthropogenic and biogenic secondary organic aerosols, Atmos. Environ., 130, 172–179, https://doi.org/10.1016/J.ATMOSENV.2015.10.019, 2016.

Scheerer, R. and Henglein, A.: The Triplet State of 3-Nitropyrene, Berichte der Bunsengesellschaft für Phys. Chemie, 81, 1234–1239, https://doi.org/10.1002/BBPC.19770811208, 1977.

Treinin, A. and Hayon, E.: Quenching of triplet states by inorganic ions. Energy transfer and charge transfer mechanisms, J. Am. Chem. Soc., 98, 3884–3891, https://doi.org/10.1021/JA00429A025, 1976.

Walhout, E. Q., Yu, H., Thrasher, C., Shusterman, J. M., and O'Brien, R. E.: Effects of photolysis on the chemical and optical properties of secondary organic material over extended time scales, ACS Earth Sp. Chem., 3, 1226–1236, https://doi.org/10.1021/ACSEARTHSPACECHEM.9B00109/SUPPL_FILE/SP9B00109_SI_002.TXT, 2019.

https://doi.org/10.5194/acp-2022-278
Preprint. Discussion started: 22 April 2022

Walser, M. L., Park, J., Gomez, A. L., Russell, A. R., and Nizkorodov, S. A.: Photochemical aging of secondary organic aerosol particles generated from the oxidation of d-limonene, J. Phys. Chem. A, 111, 1907–1913, https://doi.org/10.1021/jp066293l, 2007.

Wong, J. P. S., Zhou, S., and Abbatt, J. P. D.: Changes in secondary organic aerosol composition and mass due to photolysis: Relative humidity dependence, J. Phys. Chem. A, 119, 4309–4316, https://doi.org/10.1021/JP506898C/SUPPL_FILE/JP506898C_SI_001.PDF, 2015.

Zhao, R., Lee, A. K. Y., Huang, L., Li, X., Yang, F., and Abbatt, J. P. D.: Photochemical processing of aqueous atmospheric brown carbon, Atmos. Chem. Phys., 15, 6087–6100, https://doi.org/10.5194/ACP-15-6087-2015, 2015.

Zhou, W., Mekic, M., Liu, J., Loisel, G., Jin, B., Vione, D., and Gligorovski, S.: Ionic strength effects on the photochemical degradation of acetosyringone in atmospheric deliquescent aerosol particles, Atmos. Environ., 198, 83–88, https://doi.org/10.1016/J.ATMOSENV.2018.10.047, 2019.